Effect of the radial drift of trapped suprathermal electrons on the ECRH power deposition profile

M. Romé, U. Gasparino, H.J. Hartfuß, H. Maaßberg, N. Marushchenko †

Max-Planck Institut für Plasmaphysik
EURATOM Association, D-85748 Garching, Germany
† *Institute of Plasma Physics, NSC-KhPTI, 310108 Kharkov, Ukraine*

Introduction.

The ECRH power deposition in low density, high temperature plasmas has been analyzed at W7-AS for different heating scenarios (fundamental O-mode and second harmonic X-mode) and different magnetic configurations. These are characterized by a different size of the toroidal ripple on the magnetic axis in the toroidal position of power launching (see Fig. 1), allowing to study the influence of (toroidally) trapped particles. The analysis has been limited to the case of perpendicular, on-axis heating.
The deposition profile has been estimated from the analysis of the electron heat transport in ECRH power modulation experiments, with the time dependent electron temperatures from ECE measurements. Peaked deposition profiles are usually obtained for both heating scenarios from a 3D Hamiltonian ray-tracing code based on the assumption of Maxwellian electron distribution function (single pass absorption). The heat transport analysis predicts the same peaked absorption profiles, but additionally a much broader contribution is present, whose width and relative integral contribution with respect to the "thermal" peaked part depends on the particular heating scenario and magnetic configuration.
The effect of the magnetic configuration on the electron distribution function in the different heating scenarios being considered, has been clearly demonstrated by means of a non-linear 2D bounce-averaged Fokker-Planck (FP) code, valid for the simplified magnetic field geometry close to the magnetic axis of W7-AS [1].
In a heuristic approach, the broadening of the thermal power deposition profile is expected to be related to the radial transport (determined by the ∇B-drift) of the locally trapped suprathermal electrons generated by the ECRH. The particles drift vertically in the local magnetic ripple, becoming passing particles by pitch angle scattering, and therefore contributing to the energy flux in the outer plasma region without direct ECRH deposition, through thermalization on the flux surfaces.

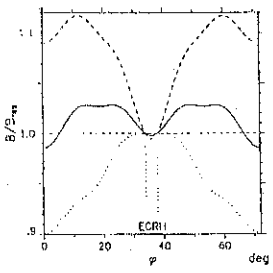

Fig. 1. *Magnetic field strength on-axis, normalized to the resonant field at the ECRH launching position, versus the toroidal angle within one field period for* $r_a \simeq 0.345$. *The solid line refers to the "standard" configuration of W7-AS, the dashed and the dotted lines correspond to the "minimum B" and the "maximum B" launching scenarios, respectively.*

Results of the power deposition analysis.

In Fig. 2a, the results of the power deposition analysis for scenarios at $B_0 = 2.5$ T in the "standard" configuration of W7-AS are summarized. The power deposition is clearly broadened for the lower densities both for fundamental O-mode (70 GHz) and for

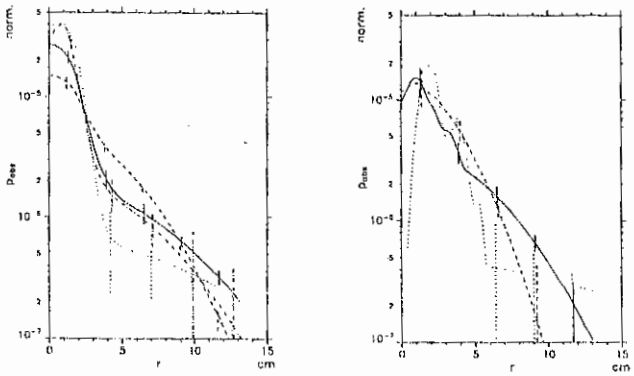

Fig. 2. *Power deposition profiles from ECRH power modulation experiments versus the effective radius r.* a: $B_0 = 2.5$ *T. The solid and the dashed lines refer to the fundamental O-mode heating (70 GHz), for* $n_e = 2 \cdot 10^{19}$ m^{-3} *and* $n_e = 10^{19}$ m^{-3}, *respectively. The dotted and the dash-dotted lines are the corresponding results for the second harmonic X-mode heating (140 GHz).* b: $B_0 = 1.25$ *T, and* $n_e = 2 \cdot 10^{19}$ m^{-3}. *The solid line refers to the "standard" configuration, the dashed and the dotted lines to the "minimum B" and the "maximum B" launching scenarios, respectively.*

second harmonic X-mode (140 GHz) launching. These findings support the picture of significant heat transport by suprathermal ripple trapped electrons since both the level of the suprathermal tail decreases and the collisional detrapping increases with density. The formation of the suprathermal tail in the ripple trapped electron distribution is expected to be more pronounced for X-mode launching [2], leading to a stronger broadening of the "effective" power deposition profile. For the O-mode scenarios, however, the lower single pass absorption and the effect of wall reflections may lead also to an enhanced broadening of the power deposition profile.

The effect of direct heating of ripple trapped electrons becomes more clear from Fig. 2b, which shows the results of a scan of the toroidal ripple, at $B_0 = 1.25$ T with second harmonic X-mode launching. In the "standard" case with 70 GHz launching, the deposition is broadened compared to the 140 GHz discharges of Fig. 2a, and this effect may be attributed to the stronger ∇B-drift of the trapped electrons. In the "maximum B" scenario, the deposition profile derived from the heat wave analysis is fairly close to the ray-tracing results, and the broadening of the deposition is of minor importance. For the "minimum B" scenario, a stronger broadening is found. All results on the power deposition are consistent with the heuristic model given above.

Convective Fokker-Planck model.

In order to simulate the broadening of the thermal power deposition profile, a simple FP model has been used, which describes the radial ∇B-drift of the toroidally trapped suprathermal electrons generated by the ECRH. In a first approach, collisional or collisionless detrapping can be treated as a loss term, i.e., the detrapped electrons are assumed to thermalize on the flux surfaces. Taking further trapping of these detrapped particles into account leads to a kind of *diffusive* modelling (with inward and outward ∇B-drifts). Neglecting this effect gives a *convective* model and the ECRH driven deviation of the trapped particle distribution from the Maxwellian defines the initial value for this *convective* FP

model. Both an analytical model and the solution of a time-dependent bounce-averaged FP code [1] are used for the initial distribution function. The drift of the suprathermal trapped electrons generated by the ECRH is described by means of the FP equation

$$< (v_{\nabla B})_z >_b \cdot \frac{\partial f_e^t}{\partial z} =< C^{lin}(f_e^t) >_b = C_w(f_e^t) + C_\lambda(f_e^t), \qquad (1)$$

where f_e^t represents the bounce-averaged distribution function of the trapped particles, $v_{\nabla B}$ the drift velocity due to the gradient of the magnetic field, and the angular brackets denote the bounce-averaging procedure, $< ... >_b \equiv \oint ...(ds/v_\parallel)/\oint(ds/v_\parallel)$, s being the coordinate along the magnetic field lines.
Stationary conditions are assumed. The presence of a radial electric field is omitted, so that the drift of the toroidally trapped electrons is mainly in the vertical direction z. The model is valid in the bulk part of the plasma axis, where the radial electric field is negligible. The collision operator is linearized by assuming a Maxwellian background. This assumption is quite reasonable outside of the ECRH deposition zone. The linearized collision operator, C^{lin}, is written as the sum of a diffusive term in $w \equiv mv^2/2T_e(z=0)$ ($\propto$ energy), and a diffusive term in $\lambda \equiv v_\perp^2 B/v^2 B_0$ ($\propto$ magnetic moment)

$$C_w(f_e^t) = \frac{2\nu_c(z)}{\sqrt{w}} \frac{\partial}{\partial w} \left\{ [2\eta(w_z) - \overline{\eta}(w_z)]\ f_e^t + \frac{T_e(z)}{T_e(0)} \sqrt{w} \frac{\partial}{\partial w} \frac{\eta(w_z)}{\sqrt{w}} f_e^t \right\},$$

$$C_\lambda(f_e^t) = 2\nu_c(z)\ \frac{\overline{\eta}(w_z) + Z_{eff}}{w^{3/2}}\ \frac{\partial}{\partial \lambda} \left[< \frac{1-\lambda\beta}{\beta} >_b\ \lambda\ \frac{\partial f_e^t}{\partial \lambda} \right],$$

respectively, with $\beta(s) \equiv B(s)/B_0$. $\nu_c(z) = \pi\sqrt{2}e^4\ n_e(z) \log\Lambda / m^{1/2} T_e^{3/2}(0)$ is the (local) collision frequency, with $\log\Lambda$ the Coulomb logarithm, $w_z = mv^2/2T_e(z)$, and

$$\eta(w_z) = \mathrm{erf}(\sqrt{w_z}) - \frac{2}{\sqrt{\pi}} \sqrt{w_z} \exp(-w_z) \quad , \quad \overline{\eta}(w_z) = \mathrm{erf}(\sqrt{w_z}) - \frac{\eta(w_z)}{2w_z}.$$

Eq. (1) is solved with difference schemes in w and λ (implicit difference formalism in z). The boundary condition $f_e^t(\lambda = \lambda_{lc}) = 0$ is used, where the function $\lambda_{lc}(z) = 1/\beta_M(z)$, represents the width of the trapped particle region, for different vertical positions z, β_M being the maximum value of the normalized magnetic field strength β. The derivative of the distribution function at the loss cone boundary, $\partial f_e^t/\partial\lambda(\lambda = \lambda_{lc})$, measures the collisional loss of the trapped electrons, while the collisionless detrapping is determined by the rate of changing of the function $\lambda_{lc}(z)$.
This model is well suited to describe the effect on the "broadening" of the ECRH power deposition profile of the loss cone size (i.e., the impact of the different magnetic field configurations), the magnetic field strength ($v_{\nabla B} \propto 1/B$), and the electron density, which enters via the initial value problem as well as via the loss rate due to collisional detrapping (the collisional slowing-down is of minor importance).

Simulations of W7-AS scenarios.
In the computations for W7-AS scenarios, the loss-cone width λ_{lc} has been assumed constant. Fig. 3a shows the power, normalized to the initial absorbed power, which is deposited at outer radii, in dependence of various parameters. The results are relevant to the "standard" configuration ($\lambda_{lc} \approx 0.97$). The behavior can be simply explained by the dependence of the ratio between the drift time, τ_D, and the collision time, $\tau_c = 1/\nu_c$, with respect to the magnetic field strength and the plasma parameters

$$\tau_D/\tau_c \propto n_e B_0 / T_e^{5/2} w^{5/2}, \qquad (2)$$

having neglected the variations with z of temperature and density, and the weak dependence of the Coulomb logarithm on the electron density. The broadening of the power

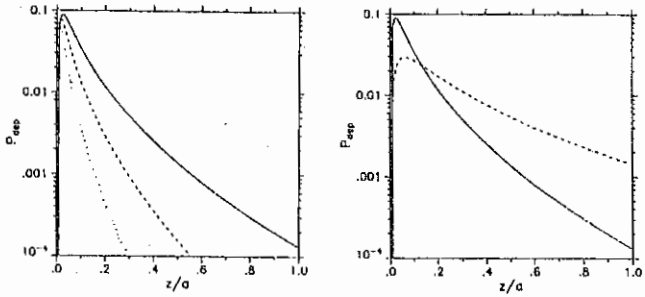

Fig. 3. *Fraction of the absorbed power deposited at the outer radii.* a: *"Standard" configuration. The solid line is the result for* $B_0 = 1.25$ *T, and* $n_e = 10^{19}$ m^{-3}, *the dashed line for* $B_0 = 2.5$ *T and* $n_e = 10^{19}$ m^{-3}, *and the dotted line for* $B_0 = 2.5$ *T and* $n_e = 2 \cdot 10^{19}$ m^{-3}. b: $B_0 = 1.25$ *T and* $n_e = 10^{19}$ m^{-3}. *The solid and the dashed lines are the results for the "standard" configuration and the "minimum B" scenario, respectively.*

deposition turns out to be larger in the case of low density and high temperature, and for decreasing magnetic field strength. Moreover, from Eq. (2) it results that the power deposition profile has a very strong dependence on the energy localization of the initial suprathermal trapped particles distribution function. The higher the velocity, where the EC resonance region is localized, the bigger is the effect of broadening of the power deposition profile.

In Fig. 3b the results for the power deposition in the case of the "standard" configuration ($\lambda_{lc} \approx 0.97$) and the "minimum B" launching ($\lambda_{lc} \approx 0.90$), are compared. Observe that for increasing loss cone width, the power is deposited on a broader radial range, and the particles could even be lost at the plasma boundary, before being thermalized. In the opposite limit of a narrow loss cone, the particles are detrapped by the pitch-angle scattering in a very short time, and in our model contribute to the power deposition only in a narrow region close to the axis. The theoretical predictions of this simplified model for the broadening of the power deposition profile, in particular its dependence on the plasma parameters and the magnetic field strength, are therefore consistent with the experimental findings.

In the case of decreasing $\lambda_{lc}(z)$, as it is the case, e.g., for the L2-stellarator, the detrapping effect of the pitch-angle scattering is weakened, so that the vertically drifting electrons remain trapped for a longer time [3]. As a consequence, less power is deposited than in the case of constant loss cone width. Depending on the rate of decreasing of λ_{lc} and on their energy, a significant fraction of the electrons may be lost at the plasma boundary. In this situation, it becomes important to take into account the presence of a radial electric field. Qualitatively, it can be observed that the effect of the electric potential is to deviate the trajectories of the particles inside the plasma, therefore increasing their confinement. Most of the absorbed power is released in any case in the central region of the plasma, with the deposition profile width being determined essentially by the initial loss cone size, and the velocity distribution.

References.

[1] N. Marushchenko *et al*, this conference
[2] M. Romé *et al.*, submitted for publication to Plasma Phys. Control. Fusion
[3] A.S. Sakharov and M.A. Tereshchenko, Plasma Phys. Rep. **21**, 93 (1995)